Life Sciences 388 (2026) 124219

Contents lists available at ScienceDirect

Life Sciences

journal homepage: www.elsevier.com/locate/lifescie

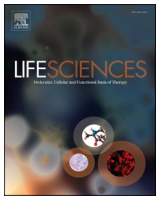

LEAP2 acts in hepatocytes and at central level, alleviates steatosis and inflammation but resistance in obese and aging

Marta V. Miguéns [a,1], Carmen Quintela-Vilariño [a,1], Sabela Casado [a,1], Tadeu de Oliveira-Diz [a], Timo D. Müller [d,e], Rubén Nogueiras [a,b,c], Carlos Diéguez [a,b], Sulay Tovar [a,b,*]

[a] Department of Physiology, Centro Singular de Investigación en Medicina Molecular y Enfermedades Crónicas (CIMUS), University of Santiago de Compostela and Instituto de Investigaciones Sanitarias de Santiago de Compostela (IDIS), Santiago de Compostela, Spain
[b] CIBER Fisiopatologia de la Obesidad y Nutrición (CIBERobn), Spain
[c] Galician Agency of Innovation (GAIN), Xunta de Galicia, Santiago de Compostela, Spain
[d] Institute for Diabetes and Obesity, Helmholtz Munich and German Center for Diabetes Research (DZD), Germany
[e] Walther-Straub-Institute for Pharmacology and Toxicology, Ludwig-Maximilians University Munich, Germany

ARTICLE INFO

Keywords:
Ghrelin
LEAP2
obesity
high fat diet
aging
steatosis
liver

ABSTRACT

Scope: Global increase in obesity and metabolic syndrome has led to a marked rise in comorbidities, with liver disease emerging as a major concern. Metabolic dysfunction-associated fatty liver disease (MAFLD) affects over 30% of the population, making it the most prevalent liver disorder worldwide. Hepatic steatosis, hallmark of MAFLD, can progress to inflammation, fibrosis, steatohepatitis, and cirrhosis. Despite advances in elucidating its mechanisms, no effective pharmacological therapy exists to reverse disease progression. Ghrelin signaling axis has been implicated in energy and lipid homeostasis, and the recent identification of liver-expressed antimicrobial peptide 2 (LEAP2) as an endogenous ghrelin receptor antagonist and inverse agonist has generated interest in its potential role in liver metabolism. The primary objective of this study was to evaluate LEAP2 on hepatocyte lipid metabolism and determine its capacity to prevent diet- and age-induced steatosis in vivo.

Methods and results: We investigated LEAP2 actions on hepatocyte lipid metabolism using human and mouse hepatocyte cultures, also we did in vivo studies in mice with chronic central LEAP2 administration in models of diet-induced and age-related steatosis.

LEAP2 inhibited lipid accumulation in hepatocytes and reduced hepatic lipid deposition in mice fed a standard diet. However, LEAP2 did not prevent high-fat diet–induced steatosis in young mice although it attenuated hepatic inflammation. In aged animals, LEAP2 failed to suppress age-associated inflammation and steatosis.

Conclusion: LEAP2 has been identified as a novel regulator of hepatic lipid metabolism with the potential to counteract inflammation-associated steatosis, although its effects on age-related steatosis appear limited. Targeting the LEAP2–ghrelin axis may represent a promising therapeutic strategy; however, further studies are required to determine its efficacy in diet-induced hepatic disease.

1. Introduction

Among the comorbidities generated because of the obesity pandemic, one of the most worrying is the development of liver pathology, which has a very high incidence in patients with metabolic syndrome. Classically, it is considered that obesity generates a process of hepatic steatosis that in later stages can progress to steatohepatitis or even fibrosis and cirrhosis [1]. Due to the limited number of therapeutic

Abbreviations: LEAP2, liver-expressed antimicrobial peptide 2; GH, Growth hormone; GHSR1a, Growth hormone secretagogue receptor 1 A; FASN, Fatty Acid Synthase; ACACA, Acetyl-CoA Carboxylase; SREBF, Sterol Regulatory Element Binding Transcription Factor 1; MLXIPL, Carbohydrate-responsive element-binding protein; CPT1α, Carnitine Palmitoyltransferase 1 A; PPARα, Peroxisome Proliferator-Activated Receptor; pIRE1α, Serine/threonine-protein kinase/endoribonuclease inositol-requiring enzyme 1 α; CHOP, C/EBP-homologous protein.

* Corresponding author at: Diabesity group, CIMUS (Centro de Investigación de Medicina Molecular y Enfermedades Crónicas), Universidade de Santiago de Compostela, Avda Barcelona s/n, 15782, Santiago de Compostela, Spain.
E-mail address: sulay.tovar@usc.es (S. Tovar).
[1] Contributed equally to this work

https://doi.org/10.1016/j.lfs.2026.124219
Received 16 September 2025; Received in revised form 15 January 2026; Accepted 19 January 2026
Available online 20 January 2026
0024-3205/© 2026 The Authors. Published by Elsevier Inc. This is an open access article under the CC BY-NC license (http://creativecommons.org/licenses/by-nc/4.0/).

options that can prevent this progressive deterioration in liver function and above all the need to have therapeutic tools that allow these processes to be reversed, uncovering the mechanisms involved that could lead to new therapies is eagerly awaited [2–4].

A key figure of liver deterioration induced by obesity is steatosis, which in turn indicates an alteration of lipid metabolism. Among the multiple signals involved in its etiopathogenesis, hepatic insulin resistance stands out. Data accumulated in recent years have also highlighted the relevance of other endocrine signals such as ghrelin. The supporting data can be summarized as follows: 1) In addition to its potent orexigenic effect, chronically elevated levels of ghrelin, acting through the Growth hormone secretagogue receptor 1a (GHSR1a), increase adiposity in white adipose tissue (WAT) and liver [5]; 2) Ghrelin receptors are expressed in hepatocytes and their in vitro activation increases lipogenesis [6]; 3) The effect of ghrelin in vivo on the liver reflect its effects on different tissues leading to an increase in the activity of enzymes involved in lipogenesis and a decrease in lipid oxidation [7]; 4) Ghrelin regulates hepatic lipogenesis de novo in a GH-independent fashion but lipid mobilization in a GH-dependent fashion as shown in GH-deficient rats [7]; 5) The signaling pathways involved in ghrelin effects on lipogenesis and lipolysis include AMP-activated protein kinase (AMPK), mechanistic target of rapamycin kinase (mTOR) and p53 [8] [9]; 6) In vivo studies carried out in animals with silencing of the ghrelin gene showed a marked resistance to the development of age-induced steatosis [10]; 7) Contradictory effects of ghrelin on steatohepatitis and liver fibrosis have been reported [11], the reason of which are unclear.

Data gleaned recently have shown that the ghrelin system is much more complex than originally envisaged since the discovery of the liver-expressed antimicrobial peptide 2 (LEAP2), as an endogenous non-competitive allosteric antagonist of the ghrelin receptor [12]. Furthermore, based on data reported in tissue databases including mRNA and protein levels it is now generally accepted that LEAP2 is synthesized in the CNS (https://www.proteinatlas.org/ENSG00000164406-LEAP2/brain). It is worth noting in this regard that LEAP2 has been shown to exert a marked inhibitory effect on the orexigenic effect and growth hormone (GH) secretion exerted by ghrelin in the hypothalamus [13]. In keeping with these opposing biological effects of ghrelin, they are also related to opposing changes in circulating levels in situations of obesity or weight loss [14,15]. Further in vivo studies in mice showed that leptin-deficient mice develop MAFLD [10] while treatment with long-acting LEAP2 led to prevention of weight loss and a decrease diet-induced liver inflammation [16]. This raised many questions regarding whether hepatic LEAP2 levels are regulated by nutrients and exposure to different diets and what are the effects of LEAP2 in vitro and in vivo in relation to hepatic lipid metabolism and on age-induced steatosis. Our data demonstrates that LEAP2 exerts an inhibitory effect on hepatic lipid accumulation through a dual mechanism. In vitro experiments revealed a direct effect of LEAP2 on hepatocytes, while in vivo studies showed that LEAP2 reduced hepatic lipid deposition and inflammation in mice fed a standard diet. However, LEAP2 failed to prevent steatosis in animals fed a high-fat diet, and in aged mice, it did not ameliorate either age-related steatosis or hepatic inflammation. These findings suggest that LEAP2 may hold therapeutic potential for metabolic-associated steatohepatitis (MASH), although its efficacy appears to depend on metabolic and physiological context.

2. Materials and methods

2.1. Cell culture

2.1.1. Human Hepatic Cell Line (HepG2)

The human hepatocellular carcinoma cell line HepG2 (European Collection of Animal Cell Cultures, 85011430) was maintained in Minimum Essential Medium Eagle (EMEM, M2279, Merck) supplemented with 10% (*v*/v) fetal bovine serum (FBS, 15377636, Gibco), 1% (v/v) Glutamine (11,500,626, Gibco)–Penicillin–Streptomycin solution (11,548,876,Gibco), and 1% (v/v) non-essential amino acids (NEAA; M7145, Merk). For experiments, HepG2 cells were seeded onto collagen type I-coated plates (collagen diluted in PBS, 1:40, C3867-1VL, Merck). Cells were cultured at 37 °C in a humidified atmosphere containing 5% CO_2. Experiments performed in HepG2 cells were carried out with n = 6–7 technical replicates per condition.

2.1.2. Isolation and culture of primary hepatocytes

Primary hepatocytes were isolated from male C57BL/6 wild-type (WT) mice fed either a standard diet (STD) or a high-fat diet (HFD) via collagenase perfusion. Hepatocytes were also obtained from GHSR WT and GHSR knockout (KO) mice. Briefly, mice were anesthetized with isoflurane, the abdomen was surgically opened, and a catheter was inserted into the inferior vena cava while the portal vein was transected. The liver was perfused with warm (37 °C) Krebs-Henseleit (KH) buffer. Following perfusion, 0.05% (*w/v*) EGTA was added to the KH buffer and perfusion continued for 5 min. Enzymatic digestion was then carried out for 10–12 min with KH buffer supplemented with Ca^{2+} and 50 mg/mL collagenase type I (LS004196, Worthington). The liver was subsequently dissociated, and viable hepatocytes were purified by density centrifugation at 500 rpm for 5 min, repeated three times at 4 °C. Purified primary hepatocytes were seeded onto collagen-coated plates at a density of 4×10^5 cells/well in adhesion medium consisting of serum-free Dulbecco's Modified Eagle Medium (DMEM) supplemented with 10% (*v*/v) FBS and 1% (v/v) Glutamine–Penicillin–Streptomycin. Experiments in primary hepatocytes were performed with n = 6 technical replicates derived from two independent hepatocyte isolations.

2.1.3. LEAP2 silencing

For RNA interference, 3.0×10^5 HepG2 cells were seeded per well in six-well plates. Cells were transfected with a pool of small-interference RNAs (siGENOME SMART Pool, Dharmacon) targeting LEAP2 or a non-targeting control siRNA (siGENOME Non-Targeting siRNA Pool, Dharmacon) using the TransIT-siQUEST reagent (Mirus). Specifically, 0.05 nmol of each siRNA diluted in 250 μL OptiMEM (31,985,070, Life Technologies) was mixed with 7.5 μL TransIT-siQUEST (pre-diluted in 243.5 μL OptiMEM), and 500 μl of this mixture was added to each well.

2.1.4. Oleic acid experiments

For experiments with oleic acid, 0.8×10^5 HepG2 cells and 0.5×10^5 primary hepatocytes were plated per well in 24-well plates. Control and LEAP2-silenced HepG2 cells were exposed to FBS-free medium supplemented with 1 mM oleic acid (MERCK) conjugated to fatty acid-free BSA (Capricorn) at a 2:1 M ratio for 24 h to induce lipid accumulation; control wells received BSA alone. Oleic acid was added 24 h after LEAP2 silencing. Separately, HepG2 and primary hepatocytes were also treated with oleic acid for 24 h and subsequently exposed to LEAP2. Lipid accumulation was assessed by Oil Red O staining.

2.1.5. Cell treatments

Cells were starved for 6 h in Krebs–Henseleit–HEPES buffer (KHH; composition: 120 mmol l-1 NaCl, 4.7 mmol l^{-1} KCl, 2.5 mmol l^{-1} $CaCl_2$, 1.2 mmol l-1 $MgSO_4$, 1.2 mmol l-1 KH_2PO_4, 25 mmol l-1 $NaHCO_3$, 25 mmol l^{-1} HEPES pH 7.4.), a fasting medium with neither nutrients nor hormones.

2.1.6. LEAP2 treatment

HepG2 cells and primary mouse hepatocytes were treated with the human LEAP2(38–77) peptide (Biorbyt) in the culture medium. HepG2 cells were exposed to 0.1 nM or 1 nM LEAP2 for 3 or 6 h, while primary hepatocytes were treated with 100 nM LEAP2 for 12 h. Dose and time conditions were selected based on preliminary dose–response experiments (data not shown). Following treatment, cells were collected for protein and mRNA extraction.

2.1.7. Viability experiments

2.1.7.1. MTT. The evaluation of cell viability in vitro was performed with a (3(4,5-dimethylthiazol-2-yl)-2,5-diphenyltetrazolium bromide) (MTT) test (M2003, MERCK). Cells were seeded in a 96 well plate at a density of 0.2×10^5cells per well. After adhesion, cells were treated with oleic acid (OA) or its control (BSA) for 24 h, then, the treatment with LEAP2 was applied to the corresponding wells. After the treatment times of 3 h and 6 h, MTT solution was diluted at 10% in cell culture medium. The cell plate medium was changed for 100 μL of medium with 10% MTT solution and cells were incubated for 30 min at 37 °C, 5% CO2. After 30 min, crystals were observed accumulating in the cells; the medium with MTT was aspirated and 100 μL DMSO was pipetted into each well.

Absorbance was measured at 570 nm wavelength. Data was normalized to the absorbance values of a basal group measured before any treatment.

2.1.7.2. Crystal violet. Cells were seeded in a 24 well plate at a density of 1.2×10^5 cells per well. After adhesion, cells were treated with oleic acid (OA) or its control (BSA) for 24 h, then, the treatment with LEAP2 was applied to the corresponding wells. After the treatment times of 3 h and 6 h, the cell medium was aspirated, and 250 μL of crystal violet staining solution was pipetted into each well. The plate was incubated at room temperature in the dark for 30 min, then each well was thoroughly washed with PBS until a soft lilac colour was achieved. Plates were left to dry in the dark for 24 h. Then pictures were taken, 500 μL of methanol was pipetted into each well and the plate was put in a shaker for 20 min. The resulting liquid was pipetted into a 96 well plate and absorbance was measured at 590 nm wavelength. Data was normalized to the absorbance values of the control group.

2.2. Animals

Adult male C57BL/6 J WT and GHSR-KO mice (Dr T.D Müller Laboratory) [17] were used. For aged mouse experiments, animals were maintained until 30 months of age. Animal experiments were conducted using n = 6–8 independent animals per group. Mice were fed either with standard chow (STD) or high-fat diet (HFD; Research Diets D12492, 60% fat, 5.24 kcal/g, Research Diets, New Brunswick, NJ) for 12 weeks. Animals were housed under controlled temperature (22–24 °C) and humidity, under a 12-h light (08:00–20:00)/12-h dark cycle, with ad libitum access to food and water. Mice were randomized by body weight immediately post-acclimatization. Animals were excluded pre-surgery for body weight loss (<15%), clinical signs (hunching, piloerection), palpable masses; post-surgery: weight-loss (<20% from baseline after 48 h surgery), persistent impairment of water and/or food intake (sustained anorexia), hypothermia (<2 °C decrease in body temperature), infection signs or general deterioration of physical condition (including piloerection, pronounced dorsal hunching, significant reduction in cardiorespiratory rate, immobility or prostration). All procedures complied with ARRIVE2.0 guidelines (https://arriveguidelines.org/arrive-guidelines). In this study, complete blinding across both the surgical procedures and downstream molecular analyses was not feasible due to the limited availability of appropriately trained personnel, which made it technically impracticable to allocate separate, independent operators for fully blinded in vivo and ex vivo phases without compromising procedural integrity or animal welfare. Importantly, the absence of blinding during the surgical phase was restricted to what was strictly necessary for practical and ethical reasons. To mitigate potential bias, all subsequent molecular and in vitro analyses were conducted using coded samples, and investigators performing these analyses were explicitly blinded to treatment groups and in vivo outcomes until all data acquisition was finalized.

Following the experimental protocols, animals were euthanized, livers were weighed and snap-frozen in dry ice, and all tissues were stored at −80 °C until analysis.

All procedures were approved by the Animal Care Research Bioethics Committee of the University of Santiago de Compostela (license 15,012/2024/005) and conducted in accordance with Directive 2010/63/EU and the Spanish Royal Decree 53/2013.

2.2.1. Central chronic LEAP2 and ghrelin treatments

For chronic intracerebroventricular (ICV) treatments, guide cannulae were stereotaxically implanted into the lateral ventricle as previously described [18]. Brain infusion cannulae were connected via catheter tubing to osmotic minipumps (Alzet, model 1007D, Durect, CA) placed subcutaneously in the interscapular region, delivering LEAP2 (10 μg/day), ghrelin (16.5 μg/day), LEAP2 plus ghrelin, or vehicle (saline) over 7 days (pump volume: 103.5 μL; flow rate: 0.51 μL/h). Surgical wounds were closed with silk sutures, and animals were allowed to recover individually in warmed cages. Body weight and food intake were monitored daily during infusion. Doses were determined based on previous studies [19–21].

After 7 days, animals were sacrificed, and tissues were rapidly harvested, snap-frozen, and stored at −80 °C. Blood samples were collected, centrifuged, and serum stored at −80 °C. For histological analysis, samples were fixed in 10% paraformaldehyde and embedded in paraffin.

2.3. Biochemical measures

LEAP2 concentrations in hepatocyte lysates and culture medium were determined by enzyme-linked immunosorbent assay (ELISA; Human LEAP2 [38–77] ELISA kit, Phoenix Pharmaceuticals) according to the manufacturer's instructions. This assay has been previously validated [22,23].

The intra- and inter-assay coefficients of variation were < 10% and < 15%, respectively, and the detection limit was 0.15 ng/mL. Absorbance was measured in duplicate at 450 nm using a microplate reader (Epoch 2, Biotek Instruments). Results are expressed as ng/mL.

2.4. Liver Triglycerides and free fatty acids content

Tissue triglycerides (TGs) and free fatty acids (FFAs) were extracted as previously described [24]. Approximately 0.05 g of liver tissue was homogenized in ice-cold chloroform:methanol (2:1, *v*/v) using a Tissue Lyser II (Qiagen) for 4 min (22 Hz), then incubated at room temperature for 3 h with rotation. Water was then added for phase separation, and samples were centrifuged; the organic layer was collected, evaporated with a SpeedVac (Thermo Fisher), and re-dissolved in chloroform. TGs (Spinreact SA, Spain, Cat #1001313) and FFAs (WAKO, Spain, Cat #436–91,995, #434–91,795) were quantified using colorimetric enzymatic assays, with each sample assayed in duplicate.

2.5. Western blot analysis

Western blotting was performed as previously described [24]. Briefly, 20 μg of total protein from tissue lysates (liver and WAT) or 8 μg from cells were resolved by SDS–PAGE and transferred to PVDF membranes (Bio-Rad). Membranes were probed with antibodies against CPT1α (ab128568, Abcam), PRDM16 (ab106410, Abcam) [25], PPARα (sc-398,394, Santa Cruz Biotechnology) [26] GRP78 (BiP, sc-13,539, Santa Cruz Biotechnology), pIRE1α (NB100-2323SS, Novus Biologicals), CHOP (sc-793, Santa Cruz Biotechnology), and PGC1α (sc-517,380, Santa Cruz Biotechnology) at 1:1000 dilution. HRP-conjugated secondary antibodies (Dako, P0448 and P0260) were used with ECL substrate (Pierce, Thermo Scientific) for visualization. X-ray films (Fuji Super RX) were developed under standard darkroom conditions. Densitometric quantification was performed using ImageJ 1.52p software, and protein levels were normalized to GAPDH for each sample and expressed relative to controls (Table 1).

Table 1
List of antibodies.

Protein Target	Manufacturer (catalog number)	Host species	Dilution
CPT1α	Abcam (ab128568)	Mouse	1:1000
PRDM16	Abcam (ab106410)	Rabbit	1:1000
PPARα	Santa Cruz Biotechnology (Sc-398,394)	Mouse	1:1000
GRP78 (BIP)	Santa Cruz Biotechnology (sc-13,539)	Rabbit	1:1000
pIRE1α	Novus Biologicals (NB100-2323SS)	Rabbit	1:1000
CHOP	Santa Cruz Biotechnology (sc-793)	Rabbit	1:1000
PGC1α	Santa Cruz Biotechnology (sc-517,380)	Mouse	1:1000
GAPDH	Merck-Millipore (CB-1001)	Mouse	1:5000
Rabbit antibodies	DAKO (P0448)	Goat	1:5000
Mouse antibodies	DAKO (P0260)	Rabbit	1:5000

2.6. Gene expression analysis

Gene expression was assessed by real-time PCR (TaqMan, Applied Biosystems, USA), as previously described [24]. Total RNA was isolated from tissues or cells using TRIzol reagent (15,596,018, Invitrogen) according to the manufacturer's instructions, followed by cDNA synthesis with the SuperScript First-Strand Synthesis System (Invitrogen) and random primers. Negative controls included reactions without template. Real-time PCR was performed in duplicate using QuantStudio 5 (Applied Biosystems) and appropriate TaqMan assays (Applied Biosystems, Life Technologies). Cycling conditions: 50 °C for 10 min, then 40 cycles of 95 °C for 15 s and 60 °C for 1 min. Relative gene expression was normalized to hypoxanthine-guanine phosphoribosyltransferase (Hprt, Mm03024075_m1) using the $2^{-\Delta\Delta Ct}$ method. TaqMan primer/probe sets (Applied Biosystems). SYBR greenreagent (Agilent Technologies) for albumin and VE-cadherin. The SYBR green cycling conditions included an initial denaturation at 95 °C for 2 min followed by 40 cycles at 95 °C for 10 s and 60 °C for 1 min, with a holding stage of 95 °C for 15 s, 60 °C for 1 min and 95 °C for 15 s. To assess the purity of primary hepatocyte cultures, hepatocyte marker (albumin) and non-parenchymal cell markers (Col1a1, F4/80, VE-cadherin) were analyzed. After normalization to GAPDH, gene expression of each gene was further expressed relative to albumin, by calculating 2ˆ-(ΔCt gene − ΔCt albumin). (Table 2)

Table 2
List of primers.

Gene ID	Reference
Hprt Mm	Taqman: Mm03024075_m1
HPRT Hs	Taqman: Hs02800695_m1
Fasn (FAS) Mm	Taqman: Mm00662319_m1
FASN (FAS) Hs	Taqman: Hs01005622_m1
Acaca (ACC) Mm	Taqman: Mm01304257_m1
ACACA (ACC) Hs	Taqman: Hs01046047_m1
Mlxipl (ChREBP) Mm	Taqman: Mm2342723_m1
MLXIPL (ChREBP) Hs	Taqman: Hs00975714_m1
Srebf1 Mm	Taqman: Mm00550338_m1
SREBF1 Hs	Taqman: Hs01088679_g1
PCK-1 Hs	Taqman: Hs00159918_m1
Scd1 Mm	Taqman: Mm00772290_m1
Tnfα Mm	Taqman: Mm00443258_m1
Adgre1 (f4/80) Mm	Taqman: Mm00802529_m1
Lgals3 (Mac-2) Mm	Taqman: Mm00802901_m1
IL6 Mm	Taqman: Mm00446190_m1
IL1b Mm	Taqman: Mm00434228_m1
Xbp1 Mm	Taqman: Mm00457357_m1
Chop (Ddit3) Mm	Taqman: Mm01135937_g1
Col1a1 Mm	Taqman: Mm00801666_g1
Primer sequence Sybr-Green	
Gapdh	**Mm Gapdh Fw** 5′- CAT CAC TGC CAC CCA GAA GAC TG −3′
	Mm Gapdh Rv 5′ - ATG CCA GTG AGC TTC CCG TTC AG −3’
Albumin	**Mm Alb FW** 5′- GAC AAG GAA AGC TGC CTG AC -3’
	Mm Alb RV 5′- TTC TGC AAA GTC AGC ATT GG −3’
VE-cadherin	**Mm VE cadherin Fw** 5’-CACTGCTTTGGGAGCCTTC-3’
	Mm VE-cadherin Rv 5’-GGGGCAGCGATTCATTTTTCT-3’

2.7. Histological procedures

2.7.1. Hematoxylin and eosin staining

Tissue samples were fixed in 10% buffered formalin for 24 h, dehydrated, and embedded in paraffin. Sections of 3 μm thickness were cut using a microtome and stained with hematoxylin and eosin by the standard alcohol-based protocol according to the manufacturer's instructions (BioOptica, Italy). Slides were mounted using a permanent, non-alcohol, non-xylene–based mounting medium. Histological sections were examined and imaged with a BX51 microscope equipped with a DP70 digital camera (Olympus, Japan).

2.7.2. Oil red O staining

Frozen liver sections (8 μm thick) were prepared using a cryostat and placed onto glass slides. Sections were fixed in 10% buffered formalin and then stained with filtered Oil Red O solution for 10 min. After staining, slides were rinsed in distilled water, counterstained with Mayer's hematoxylin for 3 min, and mounted using an aqueous mounting medium (glycerin jelly). In all the histological staining, we used up to 4 representative microphotographs of each animal were taken at 20× or 40× with a BX51 microscope equipped with a DP70 digital camera (Olympus). Oil-Red O staining was imaged under identical acquisition parameters across all samples, including objective, magnification, illumination, intensity, exposure time and camera gain). Image quantification was performed using ImageJ software (National Institutes of Health and the Laboratory for Optical and Computational Instrumentation, LOCI, University of Wisconsin). For each image, the total Oil Red O-positive area was segmented by colour-thresholding and quantified as integrated area. In parallel, the number of cells per field was determined with cell counter. Lipid content was expressed as stained area per cell by dividing the Oil Red O-positive area by the correspond cell-count. These values were then normalized to the mean of the control group and reported as relative Oil Red O staining.

2.8. Statistical analysis

Data are reported as mean ± standard error of the mean (SEM). Normality was assessed using the Anderson–Darling test, and homoscedasticity was evaluated with the Fligner–Killeen test. For comparisons across treatment groups, Statistical significance was determined by two-tailed Student's t-test or Mann-Whitney test when two groups were compared. For more than 2 groups one-way analysis of variance (ANOVA) was applied when model assumptions were met; otherwise, the Kruskal–Wallis rank-sum test was used. For longitudinal weight measurements, repeated-measures ANOVA or the Friedman rank-sum test (when normality was not satisfied) was conducted. Multiple comparisons were adjusted using the Holm method. On All statistical tests P value < 0.05 was considered statistically significant. Analyses were performed in R version 4.3.2 (R Core Team, 2023) using the statsplot package (Patil, 2021) or GraphPad Prism version 9.0 (GraphPad Software, San Diego, CA, USA).

3. Results

3.1. HepG2 cells expressed LEAP2 preventing oleic-acid induced lipid accumulation

LEAP2 expression has been reported to depend on nutritional status in both mice and humans [15,20].

To determine whether LEAP2 expression in human hepatic cells is similarly regulated, we used the HepG2 cell line and observed a decrease in LEAP2 expression following incubation with nutrient-depleted KHH medium (Fig. 1a). Conversely, under high-energy conditions, LEAP2 expression was increased after treatment with 1 mM oleic acid for 24 h (Fig. 1b). Additionally, HepG2 cells not only express but also secrete LEAP2 into the culture medium in a time-dependent and cumulative manner (Fig. 1c).

Given the established involvement of ghrelin in lipid metabolism, we hypothesized that LEAP2 may also modulate lipid accumulation. To test this, we conducted dose-response (0.1–1 nM) and time-course (3–6 h) experiments in HepG2 cells pre-treated with 1 mM oleic acid. Both concentrations of LEAP2 significantly reduced lipid droplet accumulation (Fig. 1d), with the 3-h treatment (Fig. 1d, upper panel; Fig. 1e) showing a greater effect than the 6-h treatment (Fig. 1d, lower panel; Fig. 1f), with no changes in cellular viability (Fig. 1g,h). Based on these results, we selected 0.1 nM LEAP2 and a 3-h treatment for subsequent experiments, as these conditions elicited the most pronounced reduction in lipid droplets.

Molecular analysis revealed that 0.1 nM LEAP2 for 3 h, following 24 h of oleic acid exposure, led to decreased expression of key de novo lipogenesis genes, including FASN (Fatty Acid Synthase), ACACA (Acetyl-CoA Carboxylase), SREBF (Sterol Regulatory Element Binding Transcription Factor 1), and MLXIPL (Carbohydrate-responsive element-binding protein) (Fig. 1i). At the protein level, LEAP2 treatment induced upregulation of lipolytic and lipid oxidation markers, such as CPT1α (Carnitine Palmitoyltransferase 1 A), PRDM16, and PPARα (Peroxisome Proliferator-Activated Receptor) (Fig. 1j).

Since oleic acid–induced lipid accumulation is associated with increased endoplasmic reticulum (ER) stress, we assessed whether LEAP2 modulates these pathways. LEAP2 treatment after oleic acid exposure decreased protein levels of key components of the unfolded protein response (UPR) pathway, including BiP, pIRE1α (Serine/threonine-protein kinase/endoribonuclease inositol-requiring enzyme 1 α), and CHOP (C/EBP-homologous protein), suggesting an improvement in ER stress (Fig. 1k).

To confirm the functional relevance of LEAP2, we silenced LEAP2 in HepG2 cells using specific siRNA. Knockdown efficiency was verified by ELISA in both cell lysates and culture medium (Fig. 1l). Oil Red O staining demonstrated that LEAP2-silenced cells accumulated significantly more lipids after 24 h of oleic acid exposure compared to siRNA control cells (Fig. 1m). Gene expression analysis showed a tendency toward increased FASN expression and a significant increase in PCK1 expression, further supporting a direct role for LEAP2 in regulating hepatocyte lipid accumulation (Fig. 1n). Taken together these findings imply that hepatocytes's LEAP2 synthesis and secretion are influenced by oleic acid and that LEAP2 acting in a paracrine fashion can influence hepatocyte's lipid synthesis.

3.2. LEAP2 prevents lipid accumulation in primary hepatocytes from diet-induced obese (DIO) mice

To confirm these findings in a more translational context, we isolated primary hepatocytes (with high degree of hepatocyte enrichment (Suppl Fig. 1a)) from mice fed either a high-fat diet (HFD) or standard diet (STD). Oil Red O staining demonstrated that LEAP2 treatment significantly reduced lipid accumulation in hepatocytes from HFD-fed mice (Fig. 2a). Furthermore, molecular analysis showed that hepatocytes from mice subjected to either 15 weeks (Fig. 2b) or 1 year (Fig. 2c) of HFD exhibited decreased expression of de novo lipogenesis markers (Fasn, and Acaca), which was further reduced by LEAP2 treatment in both groups. Since the relevance of GHSR expression in liver is controversial, we pursue this issue further. Of note, we demonstrated that the effect of LEAP2 is dependent on the ghrelin receptor (GHSR), as treatment with LEAP2 in primary hepatocytes isolated from GHSR knockout ($GHSR^{-/-}$) mice had no effect, as indicated by Oil Red O staining (Suppl Fig. 1b). Taken together these findings indicate that the direct effect of LEAP2 is also observed in hepatocytes derived from animals exposed to HFD and that its effect is mediated by the GHSR.

3.3. Chronic central administration of LEAP2 modulates hepatic lipid metabolism and inflammatory markers in normal-weight mice

Given the established metabolic effects of LEAP2 and the ability of central ghrelin administration to promote hepatic lipid storage and suppress lipid mobilization, we investigated the effects of central LEAP2 delivery on liver metabolism in normal-weight mice. Mice received chronic central administration of either LEAP2 or vehicle, and the impact on hepatic metabolism was assessed.

As expected, a significant difference in body weight was observed between ghrelin- and vehicle-treated groups (Fig. 3a). Histological analysis revealed no overt morphological differences between groups (Fig. 3b); however, liver weight was increased in ghrelin-treated mice and reduced in LEAP2-treated mice compared to controls (Fig. 3c). Oil Red O staining showed enhanced hepatic lipid deposition in ghrelin-treated mice, whereas lipid accumulation was attenuated following LEAP2 treatment (Fig. 3e). Biochemical analysis indicated that hepatic triglyceride levels were significantly greater in ghrelin-treated mice, while free fatty acid (FFA) levels remained unchanged among all groups (Fig. 3d).

Molecular analysis indicated that LEAP2 reduced the expression of genes involved in de novo lipogenesis, including fasn, mlxipl, and scd1 (Fig. 3f). To assess mitochondrial β-oxidation, the expression of key proteins such as CPT1α, PPARα, PGC1α, and PRDM16 was quantified (Fig. 3g). Both CPT1α and PPARα were significantly upregulated, consistent with enhanced lipid oxidation capacity.

Since the early stages of metabolic liver disease involve oxidative stress, ER stress, inflammation, and apoptosis, we explored whether LEAP2 treatment could ameliorate these processes. Notably, LEAP2 administration resulted in reduced expression of hepatic inflammatory markers, including tumor necrosis factor (tnfα) and the macrophage markers mac2 and adhesion G Protein-Coupled Receptor E1 (adgre1 (F4/80)) (Fig. 3h).

3.4. Mice with diet-induced obesity develop resistance to the effects of LEAP2 central administration in lipid accumulation

We next evaluated the effect of LEAP2 in mice fed a very high-fat diet (HFD), a regimen that induces both obesity and ghrelin resistance. As anticipated, no significant differences in body weight were observed among the groups due to ghrelin resistance (Fig. 4a). Histomorphological analysis likewise revealed no significant differences between groups (Fig. 4b), although a non-significant reduction in liver weight was noted in LEAP2-treated mice (Fig. 4c). Importantly, LEAP2 treatment did not prevent the development of hepatic steatosis, as evidenced by Oil Red O staining (Fig. 4e). While hepatic triglyceride content did not differ significantly among the groups (Fig. 4d), an increase in free fatty acids (FA) was observed in LEAP2-treated mice compared to controls.

Molecular analysis of de novo lipogenesis revealed no change in Fasn expression; however, there was a significant upregulation of Acaca, Srebf, and Mlxipl (Fig. 4f). No significant changes were detected in the expression of genes involved in mitochondrial β-oxidation (Fig. 4g). Importantly, LEAP2 treatment was also associated with reduced expression of the macrophage marker Adgre1 (F4/80) and Mac2

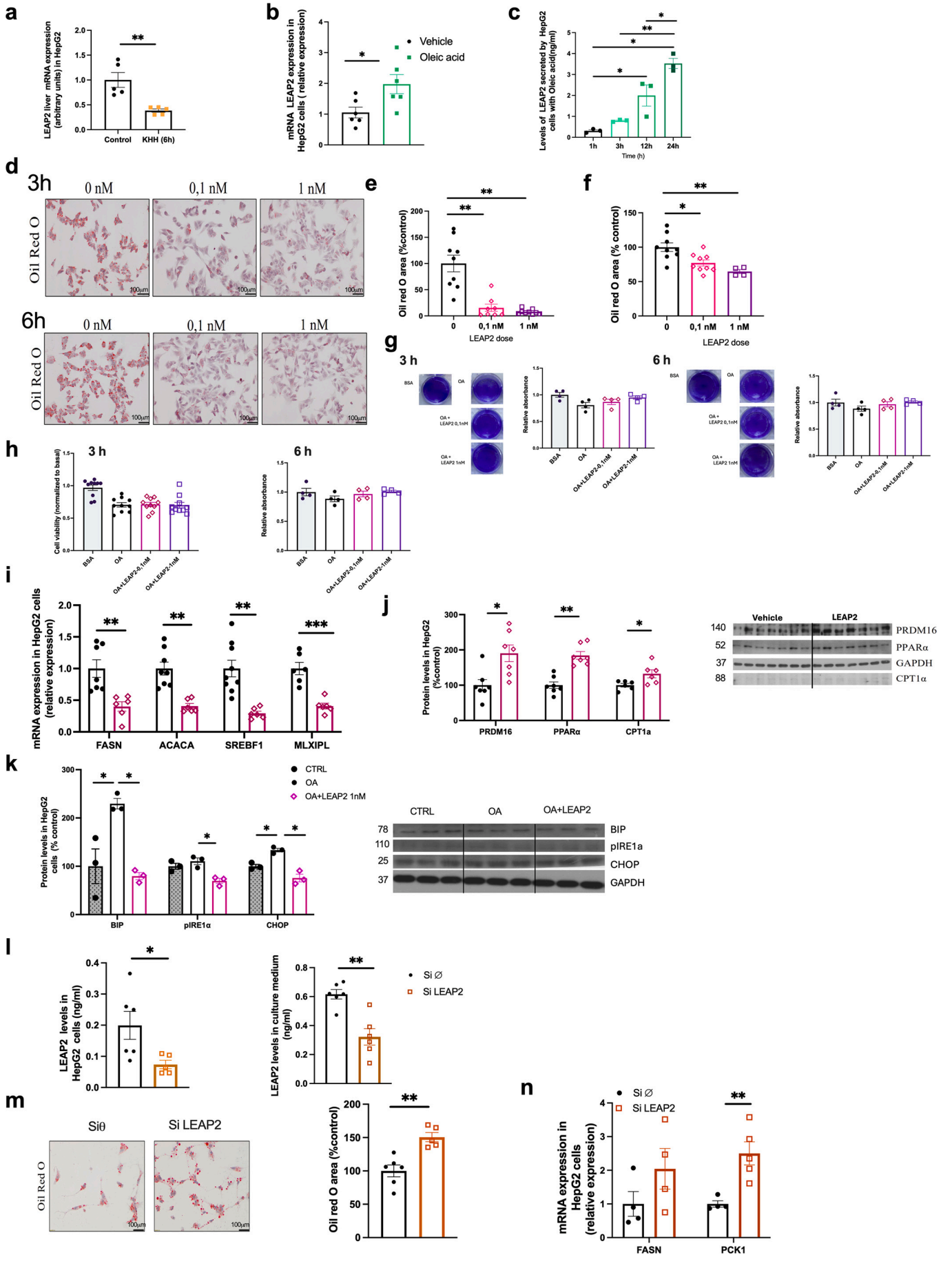

(caption on next page)

Fig. 1. *HepG2 cells expressed LEAP2 preventing oleic-acid induced lipid accumulation.* (a) LEAP2 mRNA expression in HepG2 cells. (b) LEAP2 levels and its secretion into the culture medium. (c) LEAP2 levels (ng/mL, determined by ELISA) in culture medium from HepG2 cells treated with oleic acid. (d) Representative Oil Red O staining images (scale bar = 100 μm, 20× magnification) and quantification in HepG2 cells treated with LEAP2 (0.1 nM and 1 nM) and oleic acid for 3 (e) or 6 h (f). (g) Representative images and quantification of cell viability crystal violet assay after 3 h of treatment with LEAP2 and 6 h of treatment with LEAP2 ($n = 6$–7). (h) Quantification of cell viability in MTT assay after 3 h and 6 h of treatment with LEAP2. Data was normalized to a control-non treated group ($n = 4$). (i)Analysis of FASN, ACACA, SREBF1, and MLXIPL mRNA expression after treatment with 0.1 nM LEAP2 for 3 h in medium containing oleic acid. (j) Semiquantification and representative immunoblot analysis of β-oxidation proteins (PRDM16, PPARα, CPT1α,) in HepG2 cells after treatment with 0.1 nM LEAP2 for 3 h in medium containing oleic acid. (k) Semiquantification and representative immunoblot analysis of ER stress proteins BIP, pIRE1α, and CHOP. (l) LEAP2 levels (ng/mL, measured by ELISA) in HepG2 cell extracts and culture medium after LEAP2 knockdown by siRNA. (m) Representative Oil Red O staining images (scale bar = 100 μm, 20× magnification) and semiquantification in HepG2 cells with LEAP2 silencing and 24 h treatment with 1 mM oleic acid. (n) Analysis of FASN and PCK1 mRNA expression.
Protein levels are expressed relative to the loading control GAPDH, and mRNA levels are normalized to HPRT. Data is expressed as mean ± SEM, $n = 6$–7 per group. *$p \leq 0.05$, ** $p \leq 0.01$, *** $p \leq 0.001$.

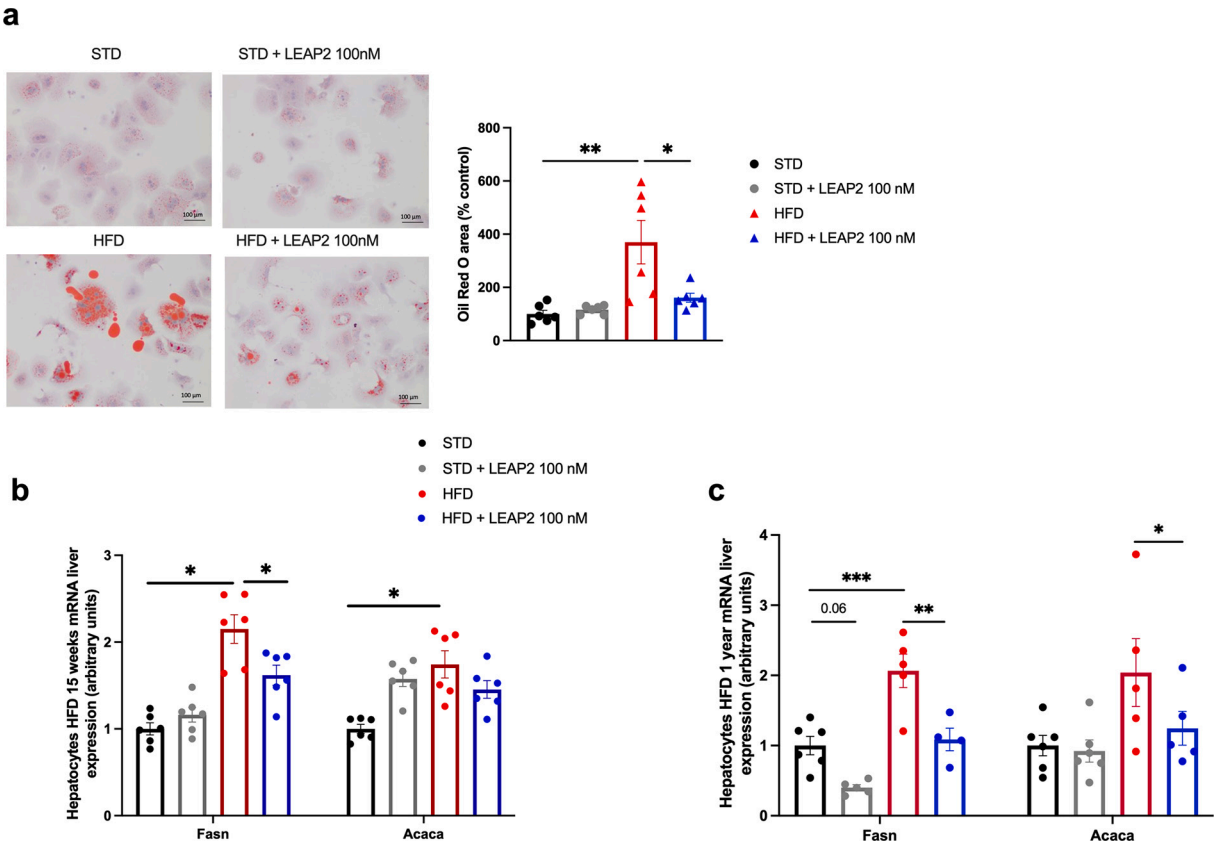

Fig. 2. *LEAP2 preventing induced lipid accumulation in primary hepatocytes from DIO mice.* (a) Representative Oil Red O staining images (scale bar = 100 μm, 20× magnification) and semiquantification in primary hepatocytes from mice fed STD diet or HFD during 15 weeks and treated with vehicle or LEAP2 (100 nM). (b) Analysis of Fasn, Acaca mRNA expression in primary hepatocytes from mice fed STD diet or HFD during 15 weeks and treated with vehicle or LEAP2 (100 nM). (c) Analysis of Fasn, Acaca mRNA expression in primary hepatocytes from mice fed STD diet or HFD during 1 year and treated with vehicle or LEAP2 (100 nM). mRNA levels are normalized to HPRT. Data is expressed as mean ± SEM, n = 6 per group. *$p \leq 0.05$, ** $p \leq 0.01$, *** $p \leq 0.001$.

(Fig. 4h) and ameliorate ER stress (Fig. 4i).

3.5. Effects of LEAP2 on aged-induced liver inflammation

Finally taking into account that liver disease reflects the consequence of different noxious stimuli, either in a sequential or simultaneous fashion, we assess the effect of LEAP2 in aged animals under chow diet. This way we have a model in which to test the effect therapeutic potential of LEAP2 in a steatosis free-model.

Mice aged 27–30 months, like "oldest-old" humans, are expected to exhibit a progressive physiological decline characterized by sarcopenia, metabolic dysfunction, immunosenescence, neuroendocrine dysregulation, and increased frailty, with substantial inter-individual variability and reduced resilience to experimental stressors. For these reasons, we carry out standard animal wellbeing biomarkers for mice such as monitoring body weight and food intake to assess weight loss or instability in food intake as well as spontaneous physical activity. Since one key feature of these animals is reduced resilience to experimental stressors, we decided against testing with stressors such as fasting, cold exposure, exercise capacity, wound healing, susceptibility to infections etc. which are commonly altered in frail individuals. As a common practice in all our experimental studies, independently of the age of the animals, all individuals exhibiting unexplained food intake and/or decreased weight loss or lack of spontaneous physical activity are discarded (data is not shown). Based on that we consider that our mice did not reach the frailty stage.

LEAP2 failed to alter basal body weight (Fig. 5a) and histological analysis revealed no differences between groups (Fig. 5b). Liver weight was unchanged under all experimental conditions (Fig. 5c) also triglyceride content (Fig. 5d). Oil Red O staining and quantification

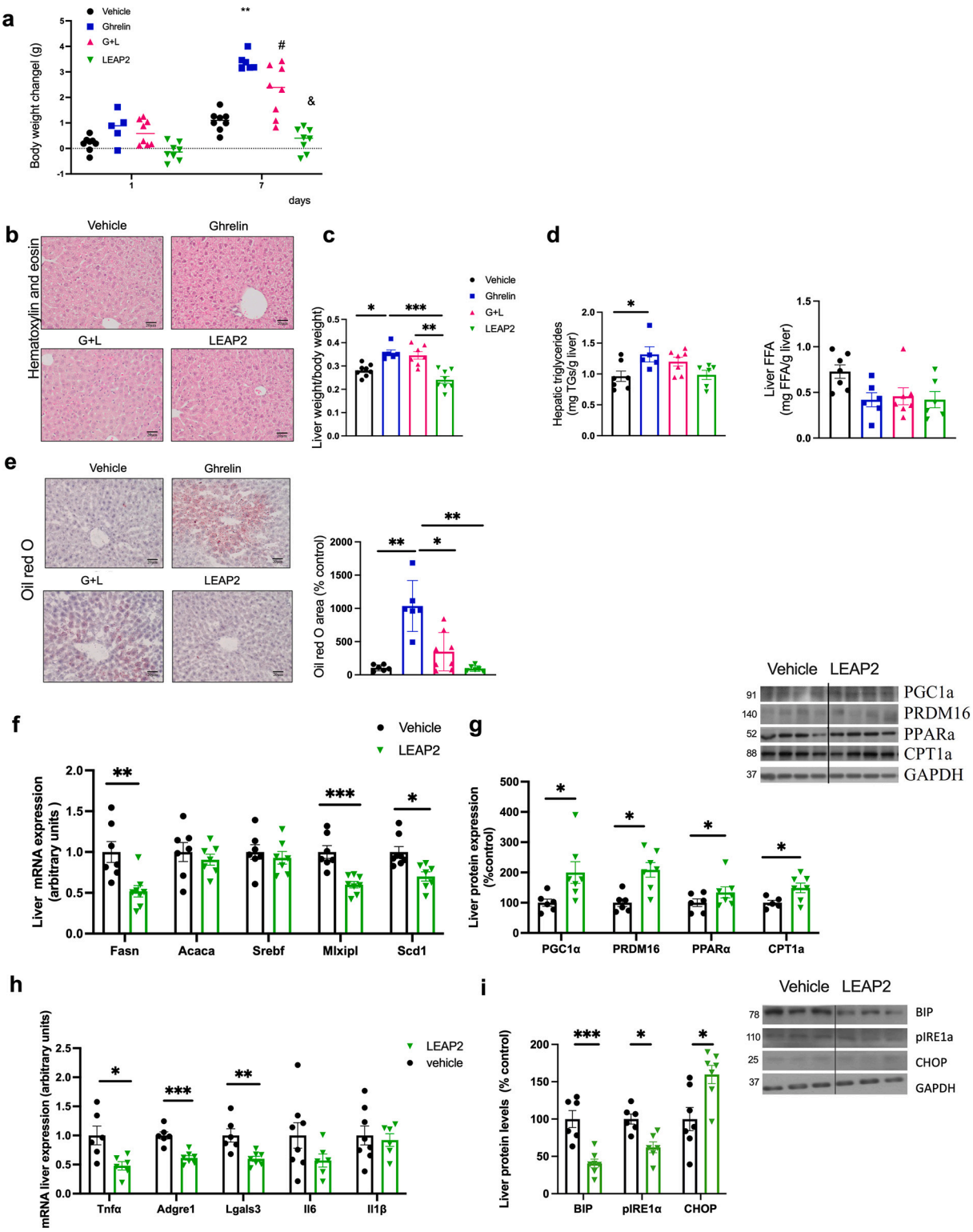

Fig. 3. *Central chronic administration of LEAP2 has effect on lipid metabolism and inflammatory markers in the liver in normal-weight mice.* (a) Body weight change in mice with administration of LEAP2, ghrelin, ghrelin and LEAP2 or vehicle during 7 days. Data is expressed as mean ± SEM *p ≤ 0.05, ** p ≤ 0.01, *** p ≤ 0.001 vehicle vs ghrelin; # $p < 0.05$, LEAP2 + ghrelin vs vehicle; & $p < 0.05$ LEAP2 vs ghrelin+LEAP2. (b) Representative Hematoxylin & Eosin staining images (scale bar = 20 μm, 10× magnification) of liver of treated mice after 7 days of treatment. (c) Liver weight. (d) Liver triglycerides and free fatty acids content after 7 days of treatment. (e) OilRed O staining images (scale bar = 20 μm, 10× magnification) and semiquantification of liver of treated mice after 7 days of treatment (f) mRNA gene expression levels of *Fasn, Acaca,Srebf, Mixipl, Scd1* in treated with vehicle or LEAP2 mice after 7 days treatment. (g) Semiquantification of immunoblot and representative blot analysis of β-oxidation proteins PGC1α, PRDM16, PPARα and CPT1a in liver after 7 days treatment (h) mRNA gene expression levels of *Tnfa, Adgre1, Lgals3, IL6, IL1b* in treated with vehicle or LEAP2 mice after 7 days treatment. (i) Semiquantification of immunoblot and representative immunoblot analysis of ER-stress proteins BIP, pIRE1α, CHOP in liver after 7 days treatment. Data is expressed as mean ± SEM, n = 6–8 per group. *p ≤ 0.05, ** p ≤ 0.01, *** p ≤ 0.001.

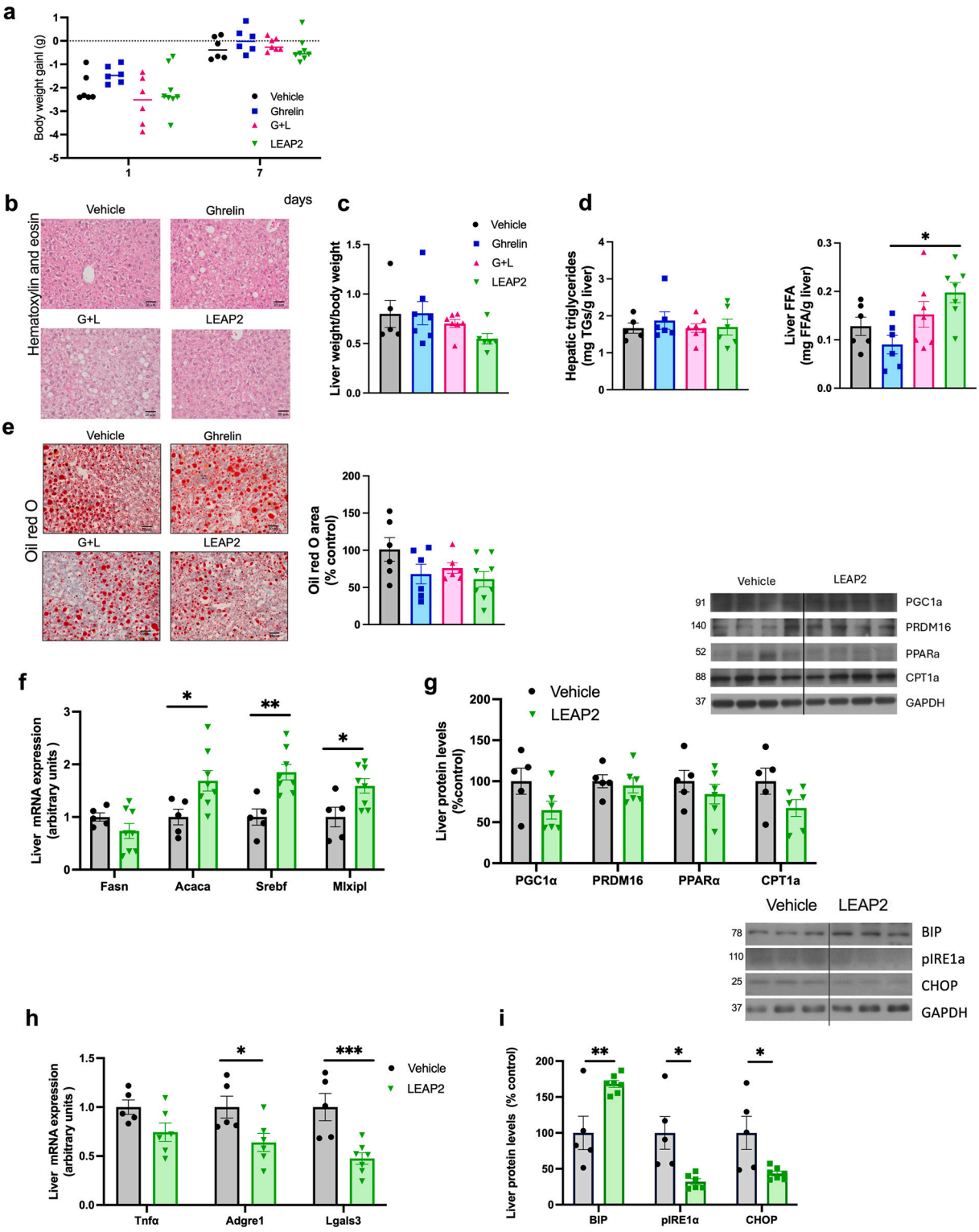

Fig. 4. *Central administration of LEAP2 in mice with diet-induced obesity showed a resistance to the effect of decreased lipid accumulation in the liver.* a) Body weight change in mice under HFD (20 weeks) with administration of LEAP2, ghrelin, ghrelin and LEAP2 or vehicle during 7 days. $N = 6–8$. Data is expressed as mean ± SEM. (b) Representative Hematoxylin & Eosin staining images (scale bar = 20 μm, 10× magnification) and weight of liver of mice under HFD and treated with LEAP2, ghrelin, ghrelin and LEAP2 or vehicle during 7 days. (c) Liver weight. (d) Liver triglycerides and free fatty acids content after 7 days of treatment. (e) Oil Red O staining images (scale bar = 20 μm) and semiquantification of liver of treated mice after 7 days of treatment (f) mRNA gene expression levels of *Fasn, Acaca,Srebf, Mixipl* in treated with vehicle or LEAP2 mice after 7 days treatment. (g) Semiquantification of immunoblot and representative immunoblot analysis of β-oxidation proteins PGC1*a*, PRDM16, PPARα and CPT1a in liver after 7 days treatment (h) mRNA gene expression levels of *Tnfa, Adgre1, Lgals3* in treated with vehicle or LEAP2 mice after 7 days treatment. (i) Semiquantification of immunoblot and representative immunoblot analysis of ER-stress proteins BIP, pIRE1α, CHOP in liver after 7 days treatment. Protein levels are expressed relative to the loading control GAPDH, and mRNA levels are normalized to HPRT. Data is expressed as mean ± SEM, n = 6–8 per group. *p ≤ 0.05, ** p ≤ 0.01, *** p ≤ 0.001.

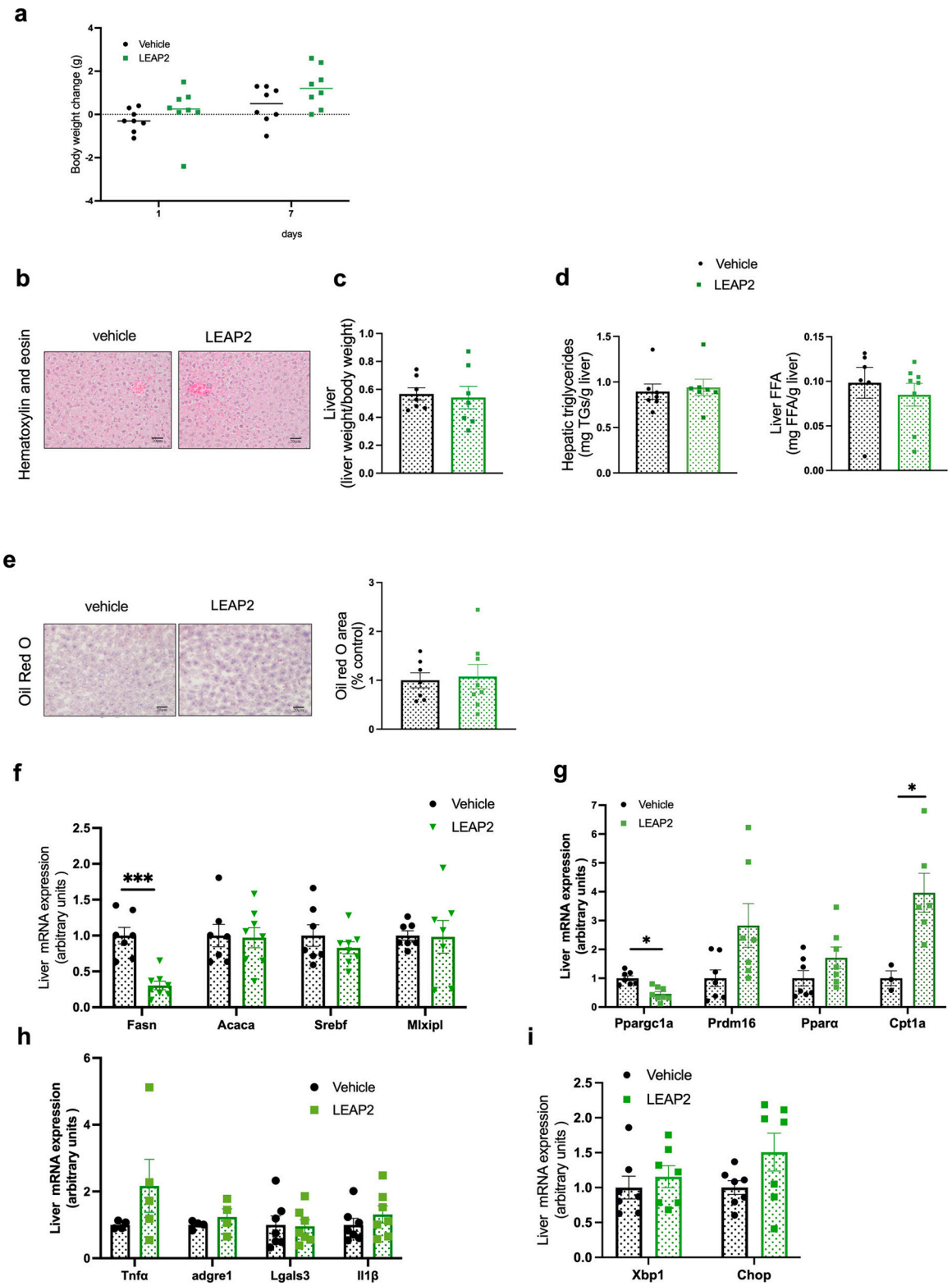

Fig. 5. *Effects on lipid metabolism in hepatic aging.* a) Body weight change in aged mice (30 months) with administration of LEAP2 or vehicle during 7 days. (b) Representative Hematoxylin & Eosin staining images (scale bar = 20 μm, 10× magnification) and weight of liver of aged mice and treated with LEAP2 or vehicle during 7 days. (c) Liver weight. (d) Liver triglycerides and free fatty acids content after 7 days of treatment. (e) Oil Red O staining images (scale bar = 20 μm, 10× magnification) and semiquantification of liver of treated mice after 7 days of treatment (f) mRNA gene expression levels of *Fasn, Acaca,Srebf, Mixipl* in treated with vehicle or LEAP2 mice after 7 days treatment. (g) mRNA gene expression levels of *Ppargc1a, Prdm16, Ppara, Cpt1a* in treated with vehicle or LEAP2 mice after 7 days treatment (h) mRNA gene expression levels of *Tnfa, Adgre1, Lgals3, IL1b* in treated with vehicle or LEAP2 mice after 7 days treatment. (i) mRNA gene expression levels of ER-stress markers Xbp1, CHOP in liver after 7 days treatment. Protein levels are expressed relative to the loading control GAPDH, and mRNA levels are normalized to HPRT. Data is expressed as mean ± SEM, $n = 7–8$ per group. *$p \leq 0.05$, ** $p \leq 0.01$, *** $p \leq 0.001$.

indicated that LEAP2-treated animals maintained hepatic lipid levels comparable to controls (Fig. 5e).

Molecular analysis showed a significant reduction in Fasn mRNA expression—a key enzyme in de novo lipogenesis—in LEAP2-treated mice compared to controls, with no significant changes detected in other lipid metabolism markers (Fig. 5f). LEAP2 treatment led to a marked increase in CPT1α protein levels and a trend toward increased PRDM16 expression but unexpectedly was associated with decreased PGC1α expression (Fig. 5g). No significant effects were observed on markers of ER stress (Fig. 5h) or inflammation (Fig. 5i), as the expression levels of the genes analyzed remained unchanged. Taken together, the changes in the expression of these markers indicate that they are not sufficient to induce a relevant change in the lipid metabolism-related phenotype.

Finally, our data shows that in this scenario, and contrary to that obtained in young animals exposed to either chow or HFD, LEAP2 failed to decrease aging-induced liver inflammation. This finding will be of relevance in relation to the development of new drugs for treatment of MASH.

4. Discussion

The possible involvement of the ghrelin system in liver function and in the development of obesity-associated comorbidities such as steatosis and steatohepatitis has been extensively investigated in recent years [27]. However, the data obtained to date do not allow for clear conclusions regarding its pathophysiological role or its potential as a therapeutic target in the context of liver disease. This uncertainty arises, in part, from the widespread expression of the ghrelin receptor both in the liver and in other tissues, centrally and peripherally [28,29].

This is particularly relevant when discussing comorbidities such as obesity, which develops largely as a consequence of altered organ crosstalk that gives rise to phenomena such as glucotoxicity, lipotoxicity, and ER stress in multiple organs, including the liver.

The complexity of the ghrelin system has been recognized since its discovery. For its principal effects—orexigenic action and GH release [30,31], acylation at a specific serine residue is required for binding to its receptor, GHSR1a [32]. Additionally, the non-acylated (unacylated) ghrelin peptide (UAG) can exert biological effects via a yet unidentified receptor distinct from GHSR1a [33] [34,35]. Complexity has further increased with the recent identification of LEAP2 as an endogenous antagonist and inverse agonist of GHSR1a. This discovery requires a reinterpretation of previously published findings on ghrelin signaling, and is of special interest because LEAP2 is synthesized in the liver [36] raising the possibility that its levels fluctuate according to the nutritional and functional state of hepatocytes. Furthermore, given the presence of GHSR1a in hepatocytes and given that this receptor exhibits constitutive activity even in the absence of ligand [37], LEAP2 may exert biological effects both in the presence and absence of ghrelin. These considerations justify the need to investigate LEAP2 actions both in vitro in hepatocytes and in vivo in animal models.

Consistent with previous reports, our data in a human hepatocyte cell line show that LEAP2 is expressed in hepatocytes, and that its expression is modulated by exposure to oleic acid. We further demonstrate that LEAP2 treatment leads to a marked reduction in lipid accumulation as well as a decrease in ER stress induced by oleic acid. In support of this, siRNA-mediated silencing of LEAP2 resulted in the opposite phenotype—namely, increased lipid accumulation. Importantly, in primary hepatocytes from mice fed a HFD, LEAP2 exerted the same protective effect as observed in the human cell line. Taken together, these data indicate that endogenous LEAP2 plays a key role in preventing hepatic steatosis. Our data also indicates that this direct effect is exerted directly in a paracrine fashion through the GHSR since it was absent in $GHSR^{-/-}$ mice.

Given the well-established metabolic actions of ghrelin at the hypothalamic level, we next explored the effects of LEAP2 on hepatic lipid metabolism in vivo in animals maintained on either standard or high-fat diets. Our data demonstrate that, in mice fed a standard diet, central ghrelin administration increased hepatic steatosis, but this effect was inhibited by LEAP2, likely through decreased de novo lipogenesis and enhanced lipid oxidation. Mechanistically, our data suggest that these LEAP2 effects are mediated by decreased ER stress and are also associated with a reduction in hepatic inflammation. Although these findings contrast with a previous study [38] in which LEAP2 knockdown improved liver steatosis—implying a pro-steatotic role for LEAP2 in that context—those authors employed a virogenic approach to reduce LEAP2. By contrast, our findings are consistent with those of Shankar et al., [39] who reported that deletion of LEAP2 in mice led to increased fat accumulation in females fed a high-fat diet, and that long-acting LEAP2 analog administration reduced body weight [40]. Furthermore, our results are supported by studies showing that chronic ghrelin administration is associated with hepatic steatosis [6,41] and that lowering circulating ghrelin improves hepatic lipid accumulation [42].

Previous studies have shown that animals fed a HFD develop resistance to ghrelin actions at the hypothalamic level [25]. We therefore evaluated the actions of LEAP2 in mice fed a HFD. Contrasting with the findings in standard-diet animals, HFD exposure induced resistance to LEAP2's actions in terms of hepatic lipid accumulation, with no significant effects observed. This was reflected by minimal alterations in markers of de novo lipogenesis or lipid oxidation. While some studies using AAV-mediated overexpression of LEAP2 in the arcuate nucleus [43] have observed hepatic effects in diet-induced obese mice, others using different genetic approaches reported ghrelin/LEAP2 resistance only in males and not females [39]. Such discrepancies likely stem from differences in experimental model, sex, and administration route. Notably, our experiments were performed exclusively in male mice, which is a limitation. Some authors have hypothesized that LEAP2 may be a determinant of ghrelin resistance [39] thus, the observation of resistance to LEAP2 under obesogenic conditions is not unexpected.

There are several mechanisms, non-mutually exclusive, that can be put forward. 1) Hypothalamic inflammation is a key feature of exposure to HFD appearing before weight gain. Resistance to ghrelin, as assessed by lack of c-fos response, appears in the course of a few days in response to microglial activation and disruption of ghrelin receptor coupling thereby failing to increase NPY/AgRP neurons [44–46] . 2) Increased levels of LEAP2 leads to a decrease in the ghrelin/LEAP2 ratio. In this context since LEAP2 is, both, a competitive antagonist and an inverse agonist, LEAP2 occupancy reduces the ghrelin signal at the receptor [12,13] . 3) Another relevant feature is that HFD leads to decrease GHSR expression in relevant neuronal populations such as the ARC in the VTA, thereby preventing LEAP2 effects [47]. 4) Ghrelin orexigenic effect is mediated by a signaling pathway which include Sirt1/p53- AMPK, CPT1c which leads to NPY-AgRP neuronal depolarization [19,48–50].

Nevertheless, our model revealed that one of the main consequences of steatosis—inflammation—was improved by LEAP2 treatment, in agreement with previous reports showing that subcutaneous administration of long-acting LEAP2 ameliorates steatosis in HFD-fed mice [16]. In contrast, an opposing pro-inflammatory effect of LEAP2 has been described in models of caloric restriction [51].

Aging is associated with impaired liver function, manifesting as both steatosis and fibrosis, which predispose to more rapid disease progression and poorer clinical outcomes. The mechanisms underpinning age-related hepatic dysfunction are diverse and include structural and functional changes within the liver, alterations in mitochondrial activity, increased cellular senescence, and metabolic imbalances such as elevated oxidative stress and reduced stress tolerance [52–54]. In light of these considerations, we examined the effect of LEAP2 on hepatic lipid metabolism in 30-month-old mice. The “oldest-old.” Mice at this life stage manifest a broad spectrum of age-associated phenotypes analogous to advanced human aging, including systemic organ dysfunction This chronological age in mice correlates approximately to humans in late senescence (exceeding 85 years of age), a demographic

classified by the British Geriatrics Society as, cognitive impairment, sarcopenia, and immunosenescence. Utilizing this model provides significant translational value for studying age-related pathologies. The selection of this specific cohort is further necessitated by global demographic shifts; current forecasts indicate that the "oldest-old" population is projected to reach nearly 500 million within the next two decades, highlighting an urgent need to understand the metabolic shifts associated with extreme longevity.

Our data indicate that aged animals are markedly resistant to the in vivo effects of LEAP2 on hepatic metabolism—as observed in young animals fed standard diet—particularly at the level of de novo lipogenesis and inflammatory markers. However, some effects on markers of lipid oxidation persist, though they are insufficient to elicit overt changes in hepatic steatosis or triglyceride content. These findings are consistent with our previous observations showing that aged mice are resistant to the effects of LEAP2 on food intake and body weight [25]. Nevertheless, in this scenario, and contrary to that obtained in young animals exposed to either chow or HFD, LEAP2 failed to decrease aging-induced liver inflammation. This finding will be of relevance in relation to the development of new drugs for treatment of MASH.

LEAP2 is produced mainly by the liver and small intestine. Leap2 mRNA levels is also detectable in brain tissue albeit at much lower levels than liver/intestine. Although detailed studies on protein expression in different neuronal populations are still lacking, it is well established that it acts centrally, when delivered intracerebroventricularly (icv) or overexpressed in hypothalamic nuclei, suppressing ghrelin actions as shown by reduced hypothalamic Fos activation, inhibition of ghrelin orexinergic effect without affecting NPY- induced food intake [20,25,39,55,56]. Of note, chemogenetic inhibition of POMC neurons abolishes LEAP2-induced hypophagia, showing POMC neurons are required for its central anorectic effects [43]. Thus, centrally acting LEAP2 (from local brain expression or circulating entry) directly modulates GHSR-expressing circuits, especially POMC neurons. Further studies, assessing LEAP2 effects following specific deletion of GHSR in different hypothalamic neuronal subtypes are needed in order to uncover the mechanisms involved in these central effects. In any case, whatever the mechanism the physiological role of LEAP2, either produced at central or peripheral level is beyond any doubt considering that genetic deletion of LEAP2 markedly influence energy and metabolic homeostasis [39].

In the context of our Ms. it should be noted that there is, at present, no definitive in vivo pharmacokinetic study showing saturable, carrier-mediated LEAP2 transport across the BBB, so the precise contribution of peripherally produced LEAP2 to brain levels remains an open question. Whether entry of LEAP2 could share a similar mechanism to ghrelin via tanycytes [57] or through fenestrated capillaries is also unknown. Therefore, the data obtained assessing the effects of intracerebroventricular (icv.) infusion of very low doses of native LEAP2, is quite robust in terms of assessing the central of LEAP2 but it does not allow to answer the relative relevance of central vs peripheral endogenous synthesized LEAP2 in the effects being described.

In summary, our data demonstrate that LEAP2 regulates hepatic lipid metabolism both directly (in vitro in human hepatocytes) and in vivo (in rodents). Importantly, the protective effect of LEAP2 observed in standard-diet-fed young mice is lost in aged animals and is similarly absent in young animals exposed to HFD. Elucidating the mechanisms underlying this resistance will improve our understanding of liver disease progression, particularly in the context of obesity and the growing population of "oldest-old" subjects.

Financial support and sponsorship

This work has been supported by grants from Ministerio de Ciencia, Innovación y Universidades-Agencia Estatal de Investigación (ST: PID2020-116741RB-I00; CD: PID2023-149533NB-I00) Xunta de Galicia (RN: ED431C2024/10), Centro de Investigación Biomédica en Red (CIBER) de Fisiopatología de la Obesidad y Nutrición (CIBERobn). CIBERobn is an initiative of the Instituto de Salud Carlos III (ISCIII) of Spain which is supported by FEDER funds.

We thank financial support from the Conselleria de Educación, Ciencia, Universidades e Formación profesional da Xunta de Galicia (Singular Research Centre accreditation ED431G/2023/02) and the European Union (European Regional Development Fund – ERDF) and Ministerio de Ciencia, Innovación y Universidades for the Maria de Maetzu Excellence Accreditation to CIMUS (CEX2024-001463-M).

CRediT authorship contribution statement

Marta V. Miguéns: Methodology, Investigation, Formal analysis. **Carmen Quintela-Vilariño:** Methodology, Investigation, Formal analysis. **Sabela Casado:** Methodology, Investigation, Formal analysis. **Tadeu de Oliveira-Diz:** Methodology. **Timo D. Müller:** Writing – review & editing, Investigation. **Rubén Nogueiras:** Writing – review & editing, Investigation. **Carlos Diéguez:** Writing – review & editing, Conceptualization. **Sulay Tovar:** Writing – original draft, Supervision, Investigation, Funding acquisition, Data curation, Conceptualization.

Declaration of competing interest

The authors declare that they have no known competing financial interests or personal relationships that could have appeared to influence the work reported in this paper.

Acknowledgments

We thank Ana Senra for the help with histological analysis.

Appendix A. Supplementary data

Supplementary data to this article can be found online at https://doi.org/10.1016/j.lfs.2026.124219.

Data availability

Data will be made available on request.

References

[1] H. Tilg, A.R. Moschen, Evolution of inflammation in nonalcoholic fatty liver disease: the multiple parallel hits hypothesis, Hepatology 52 (5) (2010) 1836–1846.
[2] N. Lazaridis, E. Tsochatzis, Current and future treatment options in non-alcoholic steatohepatitis (NASH), Expert Rev. Gastroenterol. Hepatol. 11 (4) (2017) 357–369.
[3] J.M. Schattenberg, D. Schuppan, Nonalcoholic steatohepatitis: the therapeutic challenge of a global epidemic, Curr. Opin. Lipidol. 22 (6) (2011) 479–488.
[4] B. Smeuninx, E. Boslem, M.A. Febbraio, Current and future treatments in the fight against non-alcoholic fatty liver disease, Cancers (Basel) 12 (7) (2020).
[5] M. Tschop, D.L. Smiley, M.L. Heiman, Ghrelin induces adiposity in rodents, Nature 407 (6806) (2000) 908–913.
[6] Z. Li, G. Xu, Y. Qin, et al., Ghrelin promotes hepatic lipogenesis by activation of mTOR-PPARgamma signaling pathway, Proc. Natl. Acad. Sci. U. S. A. 111 (36) (2014) 13163–13168.
[7] S. Sangiao-Alvarellos, M.J. Vazquez, L. Varela, et al., Central ghrelin regulates peripheral lipid metabolism in a growth hormone-independent fashion, Endocrinology 150 (10) (2009) 4562–4574.
[8] B. Porteiro, A. Diaz-Ruiz, G. Martinez, et al., Ghrelin requires p53 to stimulate lipid storage in fat and liver, Endocrinology 154 (10) (2013) 3671–3679.
[9] P.B. Martinez de Morentin, N. Martinez-Sanchez, J. Roa, et al., Hypothalamic mTOR: the rookie energy sensor, Curr. Mol. Med. 14 (1) (2014) 3–21.
[10] B. Guillory, N. Jawanmardi, P. Iakova, et al., Ghrelin deletion protects against age-associated hepatic steatosis by downregulating the C/EBPalpha-p300/DGAT1 pathway, Aging Cell 17 (1) (2018).
[11] S. Ezquerro, C. Tuero, S. Becerril, et al., Antagonic effect of ghrelin and LEAP-2 on hepatic stellate cell activation and liver fibrosis in obesity-associated nonalcoholic fatty liver disease, Eur. J. Endocrinol. 188 (7) (2023) 564–577.
[12] X. Ge, H. Yang, M.A. Bednarek, et al., LEAP2 Is an endogenous antagonist of the ghrelin receptor, Cell Metab. 27 (2) (2018), 461–469 e466.

[13] M. Perello, Critical insights into LEAP2 biology and physiological functions: potential roles beyond ghrelin antagonism, Endocrinology 166 (2) (2025).
[14] M.F. Andreoli, A.S. Fittipaldi, D. Castrogiovanni, et al., Pre-prandial plasma liver-expressed antimicrobial peptide 2 (LEAP2) concentration in humans is inversely associated with hunger sensation in a ghrelin independent manner, Eur. J. Nutr. 63 (3) (2024) 751–762.
[15] B.K. Mani, N. Puzziferri, Z. He, et al., LEAP2 changes with body mass and food intake in humans and mice, J. Clin. Invest. 129 (9) (2019) 3909–3923.
[16] K. Shankar, N.P. Metzger, C. Lawrence, et al., A long-acting LEAP2 analog reduces hepatic steatosis and inflammation and causes marked weight loss in mice, Mol. Metab. 84 (2024) 101950.
[17] K. Fischer, B. Finan, C. Clemmensen, L.H. van der Ploeg, M.H. Tschop, T.D. Muller, The pentapeptide RM-131 promotes food intake and adiposity in wildtype mice but not in mice lacking the ghrelin receptor, Front. Nutr. 1 (2014) 31.
[18] M. Imbernon, D. Beiroa, M.J. Vazquez, et al., Central melanin-concentrating hormone influences liver and adipose metabolism via specific hypothalamic nuclei and efferent autonomic/JNK1 pathways, Gastroenterology 144 (3) (2013), 636–649 e636.
[19] Z.B. Andrews, D.M. Erion, R. Beiler, C.S. Choi, G.I. Shulman, T.L. Horvath, Uncoupling protein-2 decreases the lipogenic actions of ghrelin, Endocrinology 151 (5) (2010) 2078–2086.
[20] J. Lugilde, S. Casado, D. Beiroa, et al., LEAP-2 counteracts ghrelin-induced food intake in a nutrient, growth hormone and age independent manner, Cells 11 (3) (2022).
[21] P.T. Pfluger, T.R. Castaneda, K.M. Heppner, et al., Ghrelin, peptide YY and their hypothalamic targets differentially regulate spontaneous physical activity, Physiol. Behav. 105 (1) (2011) 52–61.
[22] S. Barja-Fernandez, J. Lugilde, C. Castelao, et al., Circulating LEAP-2 is associated with puberty in girls, Int. J. Obes. (Lond) 45 (3) (2021) 502–514.
[23] V. Francisco, S. Tovar, J. Conde, et al., Levels of the novel endogenous antagonist of ghrelin receptor, liver-enriched antimicrobial peptide-2, in patients with rheumatoid arthritis, Nutrients 12 (4) (2020).
[24] J. Cunarro, X. Buque, S. Casado, et al., p107 Deficiency increases energy expenditure by inducing brown-fat thermogenesis and browning of white adipose tissue, Mol. Nutr. Food Res. 63 (2) (2019) e1801096.
[25] S. Casado, M. Varela-Miguens, Diz T. de Oliveira, et al., The effects of ghrelin and LEAP-2 in energy homeostasis are modulated by thermoneutrality, high-fat diet and aging, J. Endocrinol. Invest. 47 (8) (2024) 2061–2074.
[26] P. Puigserver, G. Adelmant, Z. Wu, et al., Activation of PPARgamma coactivator-1 through transcription factor docking, Science 286 (5443) (1999) 1368–1371.
[27] M. Quinones, J. Ferno, O. Al-Massadi, Ghrelin and liver disease, Rev. Endocr. Metab. Disord. 21 (1) (2020) 45–56.
[28] X.M. Guan, H. Yu, O.C. Palyha, et al., Distribution of mRNA encoding the growth hormone secretagogue receptor in brain and peripheral tissues, Brain Res. Mol. Brain Res. 48 (1) (1997) 23–29.
[29] N. Hattori, T. Saito, T. Yagyu, B.H. Jiang, K. Kitagawa, C. Inagaki, GH, GH receptor, GH secretagogue receptor, and ghrelin expression in human T cells, B cells, and neutrophils, J. Clin. Endocrinol. Metab. 86 (9) (2001) 4284–4291.
[30] L.M. Seoane, S. Tovar, R. Baldelli, et al., Ghrelin elicits a marked stimulatory effect on GH secretion in freely-moving rats, Eur. J. Endocrinol. 143 (5) (2000) R7–R9.
[31] M. Tang-Christensen, N. Vrang, S. Ortmann, M. Bidlingmaier, T.L. Horvath, M. Tschop, Central administration of ghrelin and agouti-related protein (83-132) increases food intake and decreases spontaneous locomotor activity in rats, Endocrinology 145 (10) (2004) 4645–4652.
[32] M.A. Bednarek, S.D. Feighner, S.S. Pong, et al., Structure-function studies on the new growth hormone-releasing peptide, ghrelin: minimal sequence of ghrelin necessary for activation of growth hormone secretagogue receptor 1a, J. Med. Chem. 43 (23) (2000) 4370–4376.
[33] J. Yang, M.S. Brown, G. Liang, N.V. Grishin, J.L. Goldstein, Identification of the acyltransferase that octanoylates ghrelin, an appetite-stimulating peptide hormone, Cell 132 (3) (2008) 387–396.
[34] P.J. Delhanty, S.J. Neggers, A.J. van der Lely, Des-acyl ghrelin: a metabolically active peptide, Endocr. Dev. 25 (2013) 112–121.
[35] K. Toshinai, H. Yamaguchi, Y. Sun, et al., Des-acyl ghrelin induces food intake by a mechanism independent of the growth hormone secretagogue receptor, Endocrinology 147 (5) (2006) 2306–2314.
[36] A. Englund, H. Gilliam-Vigh, M.P. Suppli, L.S. Gasbjerg, T. Vilsboll, F.K. Knop, Intestinal expression profiles and hepatic expression of LEAP2, ghrelin and their common receptor, GHSR, in humans, Peptides 177 (2024) 171227.
[37] N.D. Holliday, B. Holst, E.A. Rodionova, T.W. Schwartz, H.M. Cox, Importance of constitutive activity and arrestin-independent mechanisms for intracellular trafficking of the ghrelin receptor, Mol. Endocrinol. 21 (12) (2007) 3100–3112.
[38] X. Ma, X. Xue, J. Zhang, et al., Liver expressed antimicrobial peptide 2 is associated with steatosis in mice and humans, Exp. Clin. Endocrinol. Diabetes 129 (8) (2021) 601–610.
[39] K. Shankar, N.P. Metzger, O. Singh, et al., LEAP2 deletion in mice enhances ghrelin's actions as an orexigen and growth hormone secretagogue, Mol. Metab. 53 (2021) 101327.
[40] S.K. Holm, V.B.I. Johansen, P. Ranea-Robles, et al., Sustained weight loss with combined LEAP2 and semaglutide treatment in mice, Diabetes 74 (11) (2025) 2089–2100.
[41] M.A. Dallak, Acylated ghrelin induces but deacylated ghrelin prevents hepatic steatosis and insulin resistance in lean rats: effects on DAG/ PKC/JNK pathway, Biomed. Pharmacother. 105 (2018) 299–311.
[42] S. Zhang, Y. Mao, X. Fan, Inhibition of ghrelin o-acyltransferase attenuated lipotoxicity by inducing autophagy via AMPK-mTOR pathway, Drug Des. Devel. Ther. 12 (2018) 873–885.
[43] G. Chu, H. Peng, N. Yu, Y. Zhang, X. Lin, Y. Lu, Involvement of POMC neurons in LEAP2 regulation of food intake and body weight, Front. Endocrinol. (Lausanne) 13 (2022) 932761.
[44] N.F. Mendes, Y.B. Kim, L.A. Velloso, E.P. Araujo, Hypothalamic microglial activation in obesity: a mini-review, Front. Neurosci. 12 (2018) 846.
[45] F. Naznin, K. Toshinai, T.M. Waise, et al., Diet-induced obesity causes peripheral and central ghrelin resistance by promoting inflammation, J. Endocrinol. 226 (1) (2015) 81–92.
[46] C. Russo, M.S. Valle, A. Russo, L. Malaguarnera, The interplay between ghrelin and microglia in neuroinflammation: implications for obesity and neurodegenerative diseases, Int. J. Mol. Sci. 23 (21) (2022).
[47] D.I. Briggs, P.J. Enriori, M.B. Lemus, M.A. Cowley, Z.B. Andrews, Diet-induced obesity causes ghrelin resistance in arcuate NPY/AgRP neurons, Endocrinology 151 (10) (2010) 4745–4755.
[48] M. Lopez, R. Lage, A.K. Saha, et al., Hypothalamic fatty acid metabolism mediates the orexigenic action of ghrelin, Cell Metab. 7 (5) (2008) 389–399.
[49] L. Martins, D. Fernandez-Mallo, M.G. Novelle, et al., Hypothalamic mTOR signaling mediates the orexigenic action of ghrelin, PloS One 7 (10) (2012) e46923.
[50] D.A. Velasquez, G. Martinez, A. Romero, et al., The central Sirtuin 1/p53 pathway is essential for the orexigenic action of ghrelin, Diabetes 60 (4) (2011) 1177–1185.
[51] M.N. Islam, W. Zhang, K. Sakai, et al., Liver-expressed antimicrobial peptide 2 functions independently of growth hormone secretagogue receptor in calorie-restricted mice, Peptides 151 (2022) 170763.
[52] N.J. Hunt, S.W.S. Kang, G.P. Lockwood, D.G. Le Couteur, V.C. Cogger, Hallmarks of aging in the liver, Comput. Struct. Biotechnol. J. 17 (2019) 1151–1161.
[53] D.G. Le Couteur, M.C. Ngu, N.J. Hunt, A.E. Brandon, S.J. Simpson, V.C. Cogger, Liver, ageing and disease, Nat. Rev. Gastroenterol. Hepatol 22 (10) (2025) 680–695.
[54] C. Lopez-Otin, M.A. Blasco, L. Partridge, M. Serrano, G. Kroemer, Hallmarks of aging: an expanding universe, Cell 186 (2) (2023) 243–278.
[55] S.K. Holm, V.B.I. Johansen, C. Clemmensen, LEAP2 as a therapeutic target in obesity and cardiometabolic disorders, Rev. Endocr. Metab. Disord. 24 (2025).
[56] M.N. Islam, Y. Mita, K. Maruyama, et al., Liver-expressed antimicrobial peptide 2 antagonizes the effect of ghrelin in rodents, J. Endocrinol. 244 (1) (2020) 13–23.
[57] M. Uriarte, P.N. De Francesco, G. Fernandez, et al., Circulating ghrelin crosses the blood-cerebrospinal fluid barrier via growth hormone secretagogue receptor dependent and independent mechanisms, Mol. Cell. Endocrinol. 538 (2021) 111449.